

Cold Dark Matter detection in SUSY models at large $\tan\beta$

M. E. Gómez^{(1)*} and J. D. Vergados^{(2)†}

⁽¹⁾*Centro de Física das Interações Fundamentais (CFIF), Departamento de Física,
Instituto Superior Técnico, Av. Rovisco Pais, 1049-001 Lisboa, Portugal.*

⁽²⁾*Theoretical Physics Section, University of Ioannina,
Ioannina GR , Greece.*

Abstract

We study the direct detection rate for SUSY cold dark matter (CDM) predicted by the minimal supersymmetric standard model with universal boundary conditions and large values for $\tan\beta$. The relic abundance of the lightest supersymmetric particle (LSP), assumed to be approximately a bino, is obtained by including its coannihilations with the next-to-lightest supersymmetric particle (NLSP), which is the lightest s-tau. The cosmological constraint on this quantity severely limits the allowed SUSY parameter space, especially in the case the CP -even Higgs has mass of around 114 GeV . We find that for large $\tan\beta$ it is possible to find a subsection of the allowed parameter space, which yields detectable rates in the currently planned experiments.

*mgomez@cfif.ist.utl.pt

†vergados@cc.uoi.gr

In recent years the consideration of exotic dark matter has become necessary in order to close the Universe [1]. Furthermore in order to understand the large scale structure of the universe it has become necessary to consider matter made up of particles which were non-relativistic at the time of freeze out. This is the cold dark matter component (CDM). The COBE data [2] suggest that CDM is at least 60%. On the other hand during the last few years evidence has appeared from two different teams, the High-z Supernova Search Team [3] and the Supernova Cosmology Project [4] which suggests that the Universe may be dominated by the cosmological constant Λ . As a matter of fact recent data the situation can be adequately described by a baryonic component $\Omega_B = 0.1$ along with the exotic components $\Omega_{CDM} = 0.3$ and $\Omega_\Lambda = 0.6$.

In fact the DAMA experiment has claimed the observation of one signal in direct detection of a WIMP, which with better statistics has subsequently been interpreted as a modulation signal [5].

The above developments are in line with particle physics considerations. Thus, in the currently favored supersymmetric (SUSY) extensions of the standard model, the most natural WIMP and candidate for CDM is the LSP, i.e. the lightest supersymmetric particle. In the most favored scenarios the LSP is the lightest neutralino, which can be simply described as a Majorana fermion, a linear combination of the neutral components of the gauginos and Higgsinos [1], [6]- [11]. Its stability is guaranteed by imposing R-parity conservation, which implies that the LSP's can disappear only by annihilating in pairs. Since this particle is expected to be very massive, $m_{\tilde{\chi}} \geq 30 GeV$, and extremely non relativistic with average kinetic energy $T \leq 100 KeV$, it can be directly detected [10]- [11] mainly via the recoiling of a nucleus (A,Z) in the elastic scattering process: $\tilde{\chi} + (A, Z) \rightarrow \tilde{\chi} + (A, Z)^*$

In order to compute the event rate one needs the following ingredients:

1) An effective Lagrangian at the elementary particle (quark) level obtained in the framework of supersymmetry as described, e.g., in Refs. [1], [7] and Bottino *et al* [8].

2) A procedure in going from the quark to the nucleon level, i.e. a quark model for the nucleon. The results depend crucially on the content of the nucleon in quarks other than u and d. This is particularly true for the scalar couplings as well as the isoscalar axial coupling [12]- [14].

3) Compute the relevant nuclear matrix elements, using as reliable as possible many body

nuclear wave functions. A complete list of references can be found in recent publications [15]- [19].

In the present work we are going to be primarily concerned with the first item of the above list. We will be concerned, in particular, with SUSY models predicting a LSP with a relic abundance of cosmological interest. Following the considerations of [20] on the composition of the energy density of the universe in scenarios with vanishing and non vanishing cosmological constant we assume $\Omega_{LSP}h^2$ in the range:

$$0.09 \leq \Omega_{LSP}h^2 \leq 0.22 \quad (1)$$

Combining items 1) and 2) we can obtain the the LSP-nucleon cross section. We will limit ourselves in the experimentally interesting range:

$$4 \times 10^{-7} \text{ pb} \leq \sigma_{scalar}^{nucleon} \leq 2 \times 10^{-5} \text{ pb} \quad (2)$$

We should remember, however, that the event rate does not depend only on the nucleon cross section, but on other parameters also, mainly on the LSP mass and the nucleus used in target.

The calculation of this cross section has become pretty standard. One starts with representative input in the restricted SUSY parameter space as described in the literature, e.g. Bottino *et al.* [8], and Arnowitt *et al.* [9], [21], and recently [22].

In the present work will show how the more restrictive version of the MSSM, with minimal supergravity (mSUGRA) and gauge unification, can predict an LSP consistent with a relic abundance in the range (1) and experimentally interesting detection rates. The space of SUSY parameters compatible with a CP -even Higgs mass $m_h \approx 114$ GeV will restrict the cosmological preferred area to the region where $\tilde{\chi} - \tilde{\tau}$ coannihilations effects are sizeable.

We will consider the MSSM which described in detail in Ref. [20] and closely follow the notation as well as the renormalisation group (RG) and radiative electroweak symmetry breaking analysis of this reference. The full one-loop radiative corrections to the effective potential for the electroweak symmetry breaking and one-loop corrections to certain particle masses which have been evaluated in Ref. [23] (Appendix E) are incorporated as described in Ref. [24]. We do not impose any unification condition to the Yukawa couplings, however, even though we maintain our calculation in the large $\tan\beta$ regime. We incorporate in our

calculation the two-loop corrections to the CP-even neutral Higgs boson mass matrix by using the *FeynHiggs* subroutines Ref. [25] this improvement is significant, especially for the lighter eigenvalue, at large values of $\tan\beta$.

We restrict our a study to the case of universal soft SUSY breaking terms at the Grand Unification scale, M_{GUT} , i.e., a common mass for all scalar fields m_0 , a common gaugino mass $M_{1/2}$ and a common trilinear scalar coupling A_0 . Our effective theory below M_{GUT} then depends on the parameters ($\mu_0 = \mu(M_{GUT})$)

$$m_0, M_{1/2}, \mu_0, A_0, \alpha_G, M_{GUT}, h_t, , h_b, h_\tau, \tan\beta ,$$

where $\alpha_G = g_G^2/4\pi$ (g_G being the GUT gauge coupling constant) and h_t, h_b, h_τ are respectively the top, bottom and tau Yukawa coupling constants at M_{GUT} . The values of α_G and M_{GUT} and $|\mu_0|$ are obtained as described in Ref. [20].

For a specified value of $\tan\beta$ at the common SUSY threshold, defined as $M_S = \sqrt{m_{\tilde{t}_1} m_{\tilde{t}_2}}$, we determine h_t at M_{GUT} by fixing the top quark mass at the center of its experimental range, $m_t(m_t) = 166$ GeV. The value of h_τ at M_{GUT} is fixed by using the running tau lepton mass at m_Z , $m_\tau(m_Z) = 1.746$ GeV. We also incorporate the SUSY threshold correction to $m_\tau(M_S)$ from the approximate formula of Ref. [23].

The value of h_b at M_{GUT} is obtained such that

$$m_b(m_Z)_{SM}^{\overline{DR}} = 2.90 \pm .14 \text{ GeV} \tag{3}$$

in agreement with the experimental value given in [26]. The SUSY correction [27] to the bottom quark mass is known to increase with $\tan\beta$. This correction originates mainly from squark/gluino and squark/chargino loops and has the same sign as μ (in our convention, which is the oposite to the one used in Ref. [20,23,24]). With the values of the SUSY parameters presented in Fig. 1, the SUSY correction to m_b decreases by a 4–5% as $m_{\tilde{\chi}}$ goes from the lower to the higher value in the considered range. Following the analysis of [28], the values of eq. 3 correspond to $m_b(m_b)_{SM}^{\overline{MS}} = 4.2 \pm .2$ GeV which is in the range quoted in Ref. [29].

The choice $\mu > 0$ leads to a constraint on the parameter space coming from the lower bound on $b \rightarrow s\gamma$. As a result the relatively light vlaues for $m_{\tilde{\chi}}$ and the obtained detection rates are suppressed. From the experimental results [30] we consider a range within the 95% C.L. :

$$2.0 \times 10^{-4} < BR(b \rightarrow s\gamma) < 4.5 \times 10^{-4} \quad (4)$$

Our determination of $BR(b \rightarrow s\gamma)$ follows the procedure described in ref. [24]. However appropriate calculations for the next-to-leading order (NLO) QCD corrections to the SUSY contribution at large values of $\tan\beta$ have become available [31]. The SUSY contribution decreases as M_S increases, we found that the lower bound in (4) determines a lower limit for $m_{\tilde{\chi}}$. Therefore in order to perform a consistent prediction for $BR(b \rightarrow s\gamma)$ we have implemented the NLO QCD correction from the first Ref. [31] to the analysis described in [24].

The GUT values of $M_{1/2}$ and m_0 are traded by the value of the mass of the LSP and the mass splitting between the LSP and the NLSP (next to lightest supersymmetric particle), which in our approach is one of the $\tilde{\tau}$'s. The parameter $\Delta_{\tilde{\tau}_2} = (m_{\tilde{\tau}_2} - m_{\tilde{\chi}})/m_{\tilde{\chi}}$ is one of our basic independent parameters. This is motivated by the role played by coannihilations $\tilde{\chi} - \tilde{\tau}$ in the determination of the cosmologically preferred area of the parameter space. We keep $A_0 = 0$ in all our calculations.

The composition of the LSP on the model under consideration can be written in the basis of the gauge and Higgs bosons superpartners as:

$$\tilde{\chi} \equiv \tilde{\chi}^0 = C_{11}\tilde{B} + C_{12}\tilde{W} + C_{13}\tilde{H}_1 + C_{14}\tilde{H}_2. \quad (5)$$

In the parameter space we study, $\tilde{\chi}$ is mostly a gaugino with $P = |C_{11}|^2 + |C_{12}|^2 > .9$, with the Bino component being the most dominant one.

The parameter space considered relevant for our analysis is displayed in Fig.1. For convenience we plot the M_S , m_A and m_0 versus the the LSP mass. Since in our analysis the LSP is mostly a bino, one finds $M_{1/2} \approx 2.5m_{\tilde{\chi}}$. Two values of $\tan\beta$ were considered, one higher and one lower, which we view as representative. The higher one, $\tan\beta = 52$, corresponds approximately to the unification of the tau and top Yukawa couplings at M_{GUT} . We should clarify, however, that in making this choice we do not adhere to any particular Yukawa unification model. We find that the parameter space with this value of $\tan\beta$ is representative for the purpose of this work . The lower value, $\tan\beta = 40$, results in a $\sigma_{scalar}^{nucleon}$ smaller by one order of magnitude as we will see later. The shaded areas correspond to the range of values taken by m_A , M_S as $\Delta_{\tilde{\tau}_2}$ ranges from 0 to 1. The area associated with m_0

for the same range of $\Delta_{\bar{\tau}_2}$ is wider as shown by the dashed and solid lines. Lower values of $\tan\beta$ will tend to increase the values for m_A . This will lead to a decrease of the detection rates as we will see later.

It can be shown [17], [18], [15] that the non directional rate can be cast in the form:

$$R = \bar{R} t(a, Q_{min}) [1 + h(a, Q_{min}) \cos\alpha] \quad (6)$$

where $a = [\mu_r(A) b v_0 \sqrt{2}]^{-1}$ with b the nuclear size parameter, $\mu_r(A)$ is the LSP-nucleus reduced mass and v_0 the parameter characterizing the LSP velocity distribution assumed here to be Maxwell-Boltzmann. The quantity h describes the modulation, i.e. the dependence of the rate on the Earth's motion, which is of no interest to us in the present work. Q_{min} is the energy transfer cutoff imposed by the detector. The parameter t takes care of the folding with the LSP velocity distribution and the structure of the nucleus and it also depends on the LSP mass. The most important to us parameter is \bar{R} , which carries the essential dependence on the SUSY parameters, and it can be cast in the form:

$$\bar{R} = \frac{\rho(0)}{m_{\tilde{\chi}}} \frac{m}{Am_N} \sqrt{\langle v^2 \rangle} [\bar{\Sigma}_S + \bar{\Sigma}_{spin} + \frac{\langle v^2 \rangle}{c^2} \bar{\Sigma}_V] \quad (7)$$

Where $\rho(0)$ is the LSP density in our vicinity, which will be taken to be $0.3 \text{ GeV}/\text{cm}^3$, and m is the detector mass. $\bar{\Sigma}_i, i = S, V, spin$ are associated with the scalar, vector and spin contributions. In the present paper we will consider only the scalar contribution, which offers the best chance for measurable detection rates, in particular for medium-heavy nuclear targets, like ^{127}I . In this case

$$\bar{\Sigma}_S = \sigma_0 \mu_r^2(A) \left\{ A^2 \left[\left(f_S^0 - f_S^1 \frac{A-2Z}{A} \right)^2 \right] \simeq \sigma_{p,\chi^0}^S A^2 \left(\frac{\mu_r(A)}{\mu_r(N)} \right)^2 \right\} \quad (8)$$

where m_N is the nucleon mass, $\mu_r(N)$ is the LSP-nucleon reduced mass, σ_{p,χ^0}^S is the scalar LSP-proton cross-section and

$$\sigma_0 = \frac{1}{2\pi} (G_F m_N)^2 \simeq 0.77 \times 10^{-38} \text{ cm}^2 \quad (9)$$

The coherent scattering can be mediated via the the neutral intermediate Higgs particles (h and H), which survive as physical particles. It can also be mediated via s-quarks, via the mixing of the isodoublet and isosinlet s-quarks of the same charge. In our model we find

that the Higgs contribution becomes dominant and, as a matter of fact, the heavy Higgs H is more important (the Higgs particle A couples in a pseudoscalar way, which does not lead to coherence). As it has been pointed out in Ref. [21] large values of $\tan\beta$ and low values for the mass of the CP-even Higgs masses (m_h and m_H) enhance the Higgs exchange amplitude. This is of particular interest in our analysis, since, as $\tan\beta$ increases, the electroweak symmetry breaking imposes lower values for the pseudoscalar Higgs mass m_A (see Fig. 1). This implies a lower value for m_H . The changes on m_h are not so important, since its value can only move below an upper bound of about 120-130 GeV (see for e.g [25]). Since the values predicted for the μ -parameter also decrease, the Higgsino component of the LSP enhances the values of $\sigma_{scalar}^{nucleon}$. For all the values of the $m_{\tilde{\chi}}$, however, reported in the present work the condition $P > .9$ is maintained. It becomes even more stringent, $P > .95$, for $m_{\tilde{\chi}} > 100$ GeV.

It is well known that all quark flavors contribute, see e.g. Drees *et al* [12], since the relevant couplings are proportional to the quark masses. One encounters in the nucleon not only the usual sea quarks ($u\bar{u}, d\bar{d}$ and $s\bar{s}$) but the heavier quarks c, b, t which couple to the nucleon via two gluon exchange, see e.g. Drees *et al* [13] and references therein.

As a result one obtains an effective scalar Higgs-nucleon coupling by using effective quark masses as follows

$$m_u \rightarrow f_u m_N, \quad m_d \rightarrow f_d m_N, \quad m_s \rightarrow f_s m_N$$

$$m_Q \rightarrow f_Q m_N, \quad (\text{heavy quarks } c, b, t)$$

where m_N is the nucleon mass. The isovector contribution is now negligible. The parameters f_q , $q = u, d, s$ can be obtained by chiral symmetry breaking terms in relation to phase shift and dispersion analysis. Following Cheng and Cheng [14] we obtain

$$f_u = 0.021, \quad f_d = 0.037, \quad f_s = 0.140 \quad (\text{model B})$$

$$f_u = 0.023, \quad f_d = 0.034, \quad f_s = 0.400 \quad (\text{model C})$$

We see that in both models the s-quark is dominant. Then to leading order via quark loops and gluon exchange with the nucleon one finds:

$$f_Q = 2/27(1 - \sum_q f_q)$$

This yields:

$$f_Q = 0.060 \text{ (model B)}, \quad f_Q = 0.040 \text{ (model C)}$$

There is a correction to the above parameters coming from loops involving s-quarks [13] and due to QCD effects. Thus for large $\tan\beta$ we find [15]:

$$f_c = 0.060 \times 1.068 = 0.064, f_t = 0.060 \times 2.048 = 0.123, f_b = 0.060 \times 1.174 = 0.070$$

(model B)

$$f_c = 0.040 \times 1.068 = 0.043, f_t = 0.040 \times 2.048 = 0.082, f_b = 0.040 \times 1.174 = 0.047$$

(model B)

For a more detailed discussion we refer the reader to Refs [12,13]. With the above ingredients and employing the obtained constraints on the SUSY parameter space one can proceed to calculate first the parameter f_S^0 associated with the scalar contribution. Then combine it with the effective Higgs-quark couplings f_q and f_Q to obtain the nucleon cross section (the contribution to the scalar coupling arising from the L-R s-quark mixing is in our model negligible).

The values for $\sigma_{scalar}^{nucleon}$ for the two nucleon models described above and the input SUSY parameters presented in Fig.1 are shown in Fig. 2. As we can see nucleon model C leads to higher cross sections. For $\tan\beta = 52$ the effect of changing $\Delta_{\tilde{\tau}_2}$ (equivalently m_0 in the range shown in Fig.1) from 0 to 1 has a small effect on the cross section (not sizeable in the figure) while for $\tan\beta = 40$ the lines are widened and become bands. This effect can be understood in the light of Fig. 1. As $\tan\beta$ decreases the values of m_A (and hence m_H and the μ -parameter) increase and span a larger area as $\Delta_{\tilde{\tau}_2}$ varies from 0 to 1. This leads to a substantial decrease in the cross section for the lower value of $\tan\beta$.

The fact that $(\tilde{\chi})$ is mostly a \tilde{B} implies that the main contribution to its annihilation cross section arises from s-fermion (squark, s-lepton) exchange in the t- and u-channel leading to $f\bar{f}$ final states (f is a quark or lepton). If, however, the mass of $\tilde{\chi}$ is close to the one of the NLSP, coannihilations between the two particles must be taken into account [32]. The inclusion these coannihilation effects results in a dramatic reduction of the $(\tilde{\chi})$ relic abundance as the two lightest SUSY particles approach in mass [20,33,34]. We estimate the

relic abundance of the LSP ($\tilde{\chi}$), by employing the analysis of Ref. [20] which is appropriate for large $\tan\beta$ and includes coannihilations $\tilde{\chi} - \tilde{\tau}$, suitable for Bino like LSP. To the list of coannihilation channels of presented in [20], one should add the t-channed sneutrino exchange in the W^+W^- and H^+H^- production.

We should, at this point, clarify that in the parameter space considered here no resonances in the s-channels were found. In other words the s-channel exchange of A , h, H, Z into $\tilde{\tau}_2\tilde{\tau}_2^*$ never becomes resonant in the parameter space of our analysis. We can see in Fig. 1, however, that a line $mass = 2m_{\tilde{\chi}}$ will be above of the m_A region for the case of $\tan\beta = 52$, while for $\tan\beta = 40$ it will not. However we should emphasize here, that the position the m_A band displayed in Fig.1 respect a line of $mass = 2m_{\tilde{\chi}}$ is very sensitive to small changes in $\tan\beta$ and the values m_t, m_b and the GUT values for A_0 and m_0 . Therefore, at the large values of $\tan\beta$ it is possible to find sectors of the space of parameters where $m_A \approx m_{\tilde{\chi}}$, in these cases the the adequate treatment of the Higgs mediated anihilation channels will be determining for an accurate calculation of $\Omega_{LSP} h^2$. The choice of parameter space in the two examples we present is aimed to illustrate the decisive role of $\tan\beta$ in the LSP detection rates. In the two scenarios we choose, anihilation resonant channels are not present and coannihilations are required in order to predict a cosmologically desirable LSP relic abundance.

Fig. 3 shows the cosmologically allowed area from CDM considerations corresponding to the parameter space described in Fig.1. The $b \rightarrow s\gamma$ constraint will exclude the parameter space marked on the left of the figures. The larger range on the the values of the LSP masses corresponds to the narrow band of the mass splitting between the LSP–NLSP, which enhances the effect of coannihilations. We find the lower of the bounds of Eq. (1) in the displayed area corresponds $\Delta_{\tilde{\tau}_2} = .045$ for $\tan\beta = 52$ and $\Delta_{\tilde{\tau}_2} = .03$ for $\tan\beta = 40$, the effect of the $\tilde{\chi} - \tilde{\tau}$ coannihilation disappears for $\Delta_{\tilde{\tau}_2} \approx .25$. Higher values for $m_{\tilde{\tau}_2}$, enhance the neutralino relic abundance. We found that for values of $m_h > 105\text{GeV}$, a choice of parameters such that $m_{\tilde{\tau}_2} > 2m_{\tilde{\chi}}$ leads to values for $\Omega_{LSP} h^2 > .22$, the upper limit we consider as cosmologically desirable.

The $b \rightarrow s\gamma$ constraint is more restrictive than the bounds on the masses of the $\tilde{\tau}$ and chargino. Lines of constant mass for lighter $\tilde{\tau}$ can be easily deduced from the coordinates of the graphs in Fig. 3, the ones corresponding to values of about 95 GeV will start intersecting the cosmologically favored area in both examples, they would lay in the area excluded by

the $b \rightarrow s\gamma$ constraint. Lines of constant chargino mass would appear in the graphs of Fig. 3 as almost vertical lines. The line corresponding to $m_{\tilde{\chi}^+} = 110$ GeV will be located at $m_{\tilde{\chi}} = 64$ GeV for $\tan\beta = 52$ and $m_{\tilde{\chi}} = 62$ GeV for $\tan\beta = 40$. In the space of parameters under consideration, the difference $m_{\tilde{\chi}^+} - m_{\tilde{\chi}}$ is large enough to consider any effect of $\tilde{\chi}^+ - \tilde{\chi}$ coannihilations in the $\tilde{\chi}$ relic abundance. Other scenarios allowing sizeable $\tilde{\chi}^+ - \tilde{\chi}$ coannihilation effects may be possible for large $\tan\beta$. Such a study, however, is beyond the scope of the present work.

We find that the possible values of lightest neutral CP even Higgs mass, imposes a severe constraint on the cosmologically allowed area. We also found that, in a fashion similar to the results presented in Ref. [35] for the low $\tan\beta$ scenario, in the large $\tan\beta$ case a value of $m_h = 114$ GeV will push the cosmologically allowed area to the values of the parameters where $\tilde{\chi} - \tilde{\tau}$ coannihilations are important (see Fig. 3). Changes in the values of $\Delta_{\tilde{\tau}_2}$ will not affect significantly the values of m_h since, as we can see in the shaded areas of Fig. 1, the changes in $\Delta_{\tilde{\tau}_2}$ imply small changes on the values of m_A and M_S . Conversely small changes on m_h are translated in significative displacements of the line of constant m_h shown in Fig. 3. Indeed this line would be better understood as a band of approximately 20 GeV width on $m_{\tilde{\chi}}$ for changes on m_h from 113 GeV to 115 GeV (these changes can be understood from the shape of the curves shown, e.g, on the first reference of Ref. [25]). We can note, by observing Fig. 1, that under the conditions imposed on the parameter space larger values for $\tan\beta$ imply lower values for m_A at the same range of $m_{\tilde{\chi}}$. This helps to understand the different position of the lines of constant m_h in the two graphs of Fig. 3.

As we can see in Fig. 3, a value of $m_h = 114$ GeV will exclude the the space of parameters suitable for detection for $\tan\beta = 40$ while for $\tan\beta = 52$, the line corresponding to the same value for m_h lies inside the range of Eq. (2) for model C. The lines corresponding to $m_h = 105$ GeV would be also almost vertical lines located at the abscissa $m_{\tilde{\chi}} \approx 63$ GeV for $\tan\beta = 52$ and below the displayed area for $\tan\beta = 40$. Therefore the dependence of our conclusions on m_h is clear.

With the above ingredients one can proceed, as outlined above, with the calculation of the event rates. For a typical nucleon cross section, taken, e.g., from the set associated with $\tan\beta = 52$, exhibited in Fig. 2, we plot in Fig. 4 the event rate as a function of the LSP mass in the case of the popular target ^{127}I . Since the detector cut off energy is not so well

known, we consider two possibilities, namely $Q_{min} = 0$ and 10 KeV . The values of the quantity t , see Eq. (6), employed here have been taken from our earlier work [19]. In these plots we have excluded LSP masses less than 130 GeV to avoid a logarithmic scale. They can easily be extrapolated to values of m_{LSP} down to 100 GeV . Anyway event rates in this LSP mass region are very large in our model and it is unlikely that they would have been missed by the existing experiments.

In summary, we have found that the most popular version of the MSSM with gauge unification and universal boundary conditions at the GUT scale, and a parameter space determined by large values of $\tan\beta$, can accommodate a cosmologically suitable LSP relic abundance and predict detection rates, which can be tested in current or projected experiments.

We should mention, however, that the calculated detection rates can vary by orders of magnitude, depending on the yet unknown LSP mass. We will not be concerned here with uncertainties, which are essentially of experimental nature, like the threshold energy cut off imposed by the detector. This reduces the rates, especially for small LSP masses. In the LSP mass range considered here the reduction is about a factor of two (see Fig. 4). The next uncertainty comes from estimating the heavy quark contribution in the nucleon cross section. This seems to be under control. We take the difference between the models B and C discussed above as an indication of such uncertainties. They seem to imply uncertainties no more than factors of two (see Fig. 2). The nuclear uncertainties for the coherent process are even smaller.

We believe, therefore, that, concerning the direct LSP detection event rates the main uncertainties come from the fact that the SUSY parameter space is not yet sufficiently constrained. The parameter space may be sharpened by the accelerator experiments, even if the LSP is not found. We should mention here, in particular, the Higgs searches, since, as we have seen, the role of the Higgs particles in direct SUSY dark matter detection is crucial. It is not an exaggeration to say that the underground and accelerator experiments are complementary and should achieve a symbiosis.

Note added: After the first version of this work was completed the Muon ($g - 2$) Collaboration had published a new measurement of the anomalous magnetic moment of the muon [36]. The result presented differs from the SM prediction by 2.6σ . If this discrepancy

is attributed to SUSY contributions, the $(g - 2)$ may impose a further constraint on the parameter space presented here. When we consider the reported discrepancy at the $2 - \sigma$ level as the allowed range for the SUSY contribution, the values we found do not have a significant impact in the parameter space considered in this work. Using the calculation presented in ref. [37] the upper bound will exclude mostly the area already excluded by $b \rightarrow s\gamma$, while the area excluded by the lower bound corresponds to values of $m_{\tilde{\chi}} > 300\text{GeV}$. We are thus in agreement with Ref. [38] in the space of parameters we overlap.

We would like to thank S. Khalil for useful discussions and for reading the manuscript and T. Falk for pointing out the missing coannihilation channels on the list of Ref. [20]. M.E.G. thanks the University of Ioannina for kind hospitality. This work was supported by the European Union under TMR contract No. ERBFMRX-CT96-0090 and ΠΕΝΕΔ 95 of the Greek Secretariat for Research.

REFERENCES

- [1] For a recent review see e.g. G. Jungman *et al.*, *Phys. Rep.* **267**, 195 (1996).
- [2] G.F. Smoot *et al.*, (COBE data), *Astrophys. J.* **396** (1992) L1.
- [3] A.G. Riess *et al.*, *Astron. J.*; **116** (1998), 1009; M.A.K. Gross, R.S. Somerville, J.R. Primack, J. Holtzman and A.A. Klypin, *Mon. Not. R. Astron. Soc.* **301**, 81 (1998).
- [4] S. Perlmutter, M.S. Turner and M. White, *Phys. Rev. Lett.* **83**, 670 (1999);. Perlmutter, S. *et al* *Astrophys. J.* **517**,565; (1997) **483**,565 (*astro-ph/9812133*); R.S. Somerville, J.R. Primack and S.M. Faber, *astro-ph/9806228*; *Mon. Not. R. Astron. Soc.* (in press).
- [5] R. Bernabei *et al.*, *Phys. Lett.* **B 389**, 757 (1996); R. Bernabei *et al.*, *Phys. Lett.* **B 424**, 195 (1998); **B 450**, 448 (1999).
- [6] H. Goldberg, *Phys. Rev. Lett* **50**, 1419 (1983); M.W. Goodman and E. Witten, *Phys. Rev.* **D 31**, 3059 (1985); K. Griest, *Phys. Rev. Lett* **61**, 666 (1988); *Phys. Rev.* **D 38**, 2357 (1988) ; **D 39**, 3802 (1989); J. Ellis, and R.A. Flores, *Phys. Lett.* **B 263**, 259 (1991); *Phys. Lett* **B 300**, 175 (1993); *Nucl. Phys.* **B 400**, 25 (1993); J. Ellis and L. Roszkowski, *Phys. Lett.* **B 283**, 252 (1992).
- [7] H.E. Haber and G.L.Kane, *Phys. Rep.* **117**, 75 (1985).
- [8] A. Bottino *et al.*, *Mod. Phys. Lett.* **A 7**, 733 (1992); *Phys. Lett.* **B 265**, 57 (1991); *Phys. Lett* **B 402**, 113 (1997); Z. Berezhinsky *et al.*, *Astroparticle Phys.* **5**, 1 (1996); V.A. Bednyakov, H.V. Klapdor-Kleingrothaus and S.G. Kovalenko, *Phys. Lett.* **B 329**, 5 (1994).
- [9] R. Arnowitt and P. Nath, *hep-ph/9701301*; *hep-ph/9902237*; P. Nath, R. Arnowitt and A.H. Chamseddine, *Nucl. Phys.* **B 227**, 121 (1983); R. Arnowitt and P. Nath, *Mod. Phys. Lett.* **10**, 1215 (1995); R. Arnowitt and P. Nath, *Phys. Rev. Lett.* **74**, 4952 (1995); R. Arnowitt and P. Nath, *Phys. Rev.* **D 54**, 2394 (1996). S.K. Soni and H.A. Weldon, *Phys. Lett.* **B 126**, 215 (1983); V.S. Kapunovsky and J. Louis, *Phys. Lett.* **B 306**, 268 (1993); M. Drees, *Phys. Lett* **B 181**, 279 (1986); P. Nath and R. Arnowitt, *Phys. Rev.* **D 39**, 279 (1989); J.S. Hagelin and S. Kelly, *Nucl. Phys.* **B 342**, 95 (1990); Y. Kamamura, H. Murayama and M. Yamaguchi, *Phys. Lett.* **B 324**, 52 (1994); S. Dimopoulos and H. Georgi, *Nucl. Phys.* **B 206**, 387 (1981).
- [10] J.D. Vergados, *J. of Phys.* **G 22**, 253 (1996).

- [11] T.S. Kosmas and J.D. Vergados, *Phys. Rev.* **D 55**, 1752 (1997).
- [12] M. Drees and M.M. Nojiri, *Phys. Rev.* **D 48**, 3843 (1993); *Phys. Rev.* **D 47**, 4226 (1993).
- [13] A. Djouadi and M. Drees, TUM-HEP-370-00;PM/00-14; S. Dawson, *Nucl. Phys.* **B359**,283 (1991) M. Spira et al, *Nucl. Phys.* **B453**,17 (1995)
- [14] T.P. Cheng, *Phys. Rev.* **D 38** 2869 (1988); H -Y. Cheng, *Phys. Lett.* **B 219** 347 (1989).
- [15] J.D. Vergados, hep-ph/0010151.
- [16] P.C. Divari, T.S. Kosmas, J.D. Vergados and L.D. Skouras, *Phys. Rev.* **C 61**,054612 (2000).
- [17] J.D. Vergados, *Phys. Rev.* **D 58**, 103001-1 (1998).
- [18] J.D. Vergados, *Phys. Rev. Lett* **83**, 3597 (1999).
- [19] J.D. Vergados, *Phys. Rev.* **D 62**, 023519-1 (2000). *Phys. Rev.* **C 61** (2000), 044612-1.
- [20] M. Gómez, G. Lazarides and C. Pallis, *Phys. Rev.* **D61** (2000) 123512.
- [21] A. Botino, F. Donato, N. Fornengo and S. Scopel, *Phys. Rev.* **D59** (1999) 095004; *Phys. Rev.* **D59** (1999) 095003.
- [22] A. Botino, F. Donato, N. Fornengo and S. Scopel, hep-ph/0010203; E. Accomando, R. Arnowitt, B. Dutta, Y. Santoso *Nucl.Phys.*B585:124-142,2000; J. Ellis, A. Ferstl, K. A. Olive, *Phys.Lett.*B481:304-314,2000; and hep-ph/0007113; J.L Feng, K.T. Matchev and F. Wilczek, hep-ph/0004043; E. Gabrielli, S. Khalil, C. Muñoz and E. Torrente-Lujan,hep-ph/0006266; V. Mandic, A. Pierce, P. Gondolo and H. Murayama, hep-ph/0008022;
- [23] D. Pierce, J. Bagger, K. Matchev and R. Zhang, *Nucl. Phys.* **B491** (1997) 3.
- [24] M. Gómez, G. Lazarides and C. Pallis, *Phys. Lett.* **B487** (2000) 313.
- [25] S. Heinemeyer, W. Hollik and G. Weiglein, hep-ph/0002213; *Comput.Phys.Commun.* 124 (2000) 76-89, hep-ph/9812320.
- [26] S. Martí i Gracia, J. Fuster and S. Cabrera, *Nucl. Phys. (Proc. Sup.)* **B64** (1998) 376.
- [27] L. Hall, R. Rattazzi and U. Sarid, *Phys. Rev.* **D50** (1994) 7048; R. Hempfling, *Phys. Rev.* **D49** (1994) 6168.
- [28] K. G. Chetyrkin, *Phys. Lett.* **B404** (1997) 161; F.A. Chishtie and V. Elias, hep-ph/0012254;
- [29] *Review of particle Physics*, D.E. Groom et al., *Eur. Phys. J.* **C15** (2000) 1; F.I. Yndurain, *Nucl. Phys. (Proc. Sup.)* **B93** (2001) 196.

- [30] CLEO Collaboration S. Glenn *et al.*, CLEO CONF 98–17, talk presented at the XXIX ICHEP98, UBC, BC Vancouver, Canada, July 23-29, 1998; ALEPH Collaboration R. Barate *et al.* Phys. Lett. **B429** (1998) 169.
- [31] C. Degrandi, P. Gambino and G. F. Giudice, JHEP **0012** (2000) 009; M. Carena, D. García, U. Nierste and C. E. Wagner, Phys. Lett. **B499** (2001) 141;
- [32] K. Griest and D. Seckel, Phys. Rev. **D43** (1991) 3191.
- [33] M. Drees and M. M. Nojiri, Phys. Rev. **D47** (1993) 376; S. Mizuta and M. Yamaguchi, Phys. Lett. **B298** (1993) 120; P. Gondolo and J. Edsjö, Phys. Rev. **D56** (1997) 1879; M. Drees, hep-ph/9703260;
- [34] J. Ellis, T. Falk and K. A. Olive, Phys. Lett. **B444** (1998) 367; J. Ellis, T. Falk, G. Ganis, K. A. Olive and M. Schmitt, Phys. Rev. **D58** (1998) 095002; J. Ellis, T. Falk, K. A. Olive and M. Srednicki, Astropart. Phys. **13** (2000) 181; J. Ellis, G. Ganis and K. A. Olive, Phys. Lett. **B474** (2000) 314.
- [35] J. Ellis, G. Ganis, D.V. Nanopoulos and K.A. Olive, hep-ph/0009355
- [36] H. N. Brown *et al.*, hep-ex/0102017.
- [37] J. Hisano, T. Moroi, K. Tobe and M. Yamaguchi, Phys. Rev. **D53** (1996) 2442;
- [38] J. Ellis, D.V. Nanopoulos and K. A. Olive, hep-ph/0102331.

FIGURES

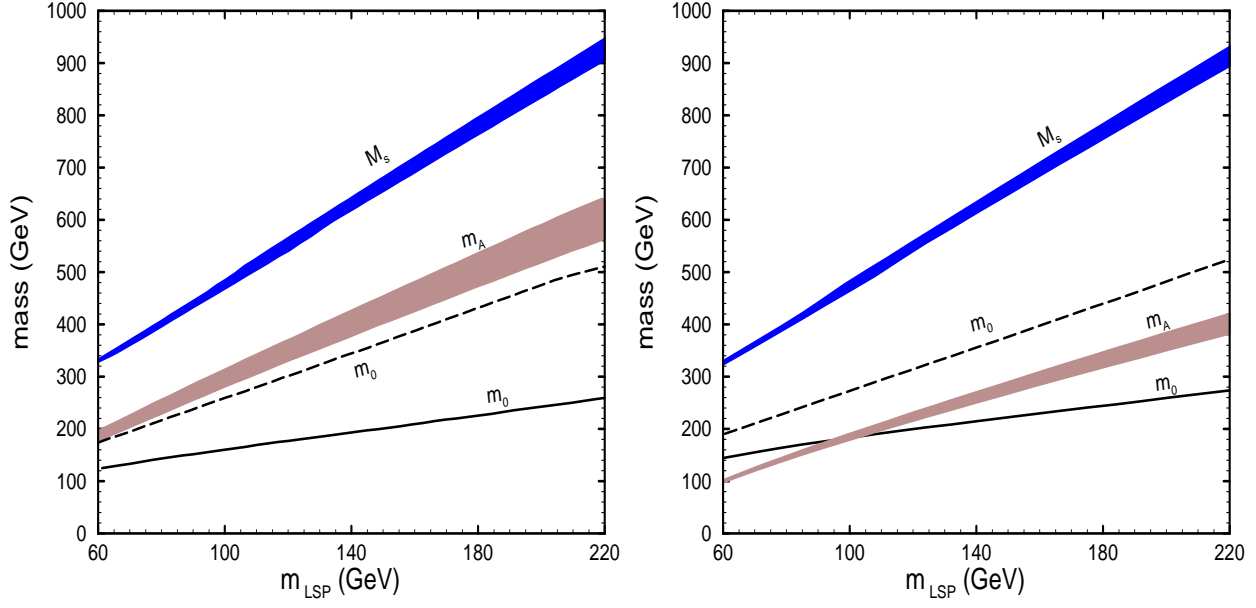


FIG. 1. The values of m_0 , m_A and M_S as functions of $m_{\tilde{\chi}}$ or $m_{\tilde{\chi}}$ for $\tan\beta = 40$ (left) and $\tan\beta = 52$ (right), $\mu > 0$, $A_0 = 0$, the upper boundaries (lower) on the shaded areas and the upper (lower) dashed line corresponds to $m_{\tilde{\tau}_2} = 2 \times m_{\tilde{\chi}}$ ($m_{\tilde{\tau}_2} = m_{\tilde{\chi}}$).

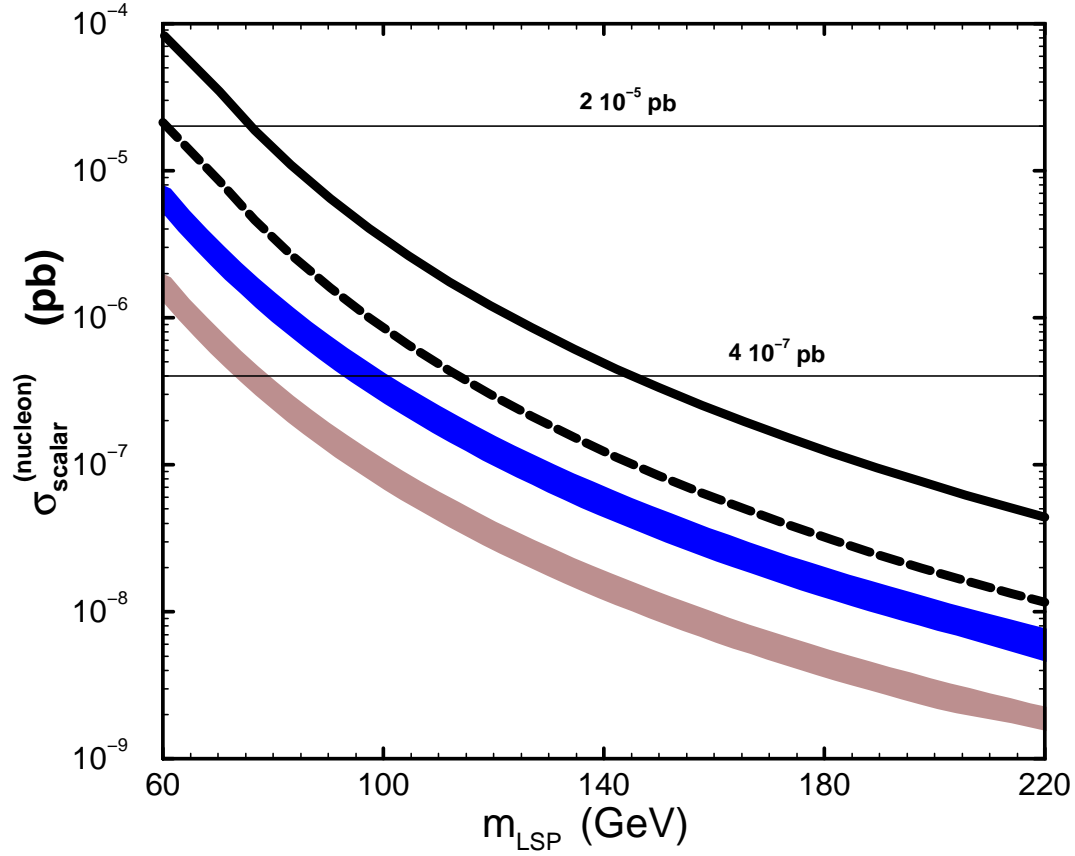


FIG. 2. Values for $\sigma_{scalar}^{(nucleon)}$, corresponding to the input parameters presented in Fig. 1. The upper lines corresponds to $\tan \beta = 52$, the solid (dashed) one was obtained using model C (B). The effect of changing with $\Delta_{\tilde{\tau}_2}$ from 0 to 1 is not sizeable for $\tan \beta = 52$. The bands are obtained using $\tan \beta = 40$, the darker shaded band corresponds to model C with the upper bound corresponding to $\Delta_{\tilde{\tau}_2} = 1$ and the lower to $\Delta_{\tilde{\tau}_2} = 0$. The light shaded band corresponds to model B, for the same range of values of $\Delta_{\tilde{\tau}_2}$

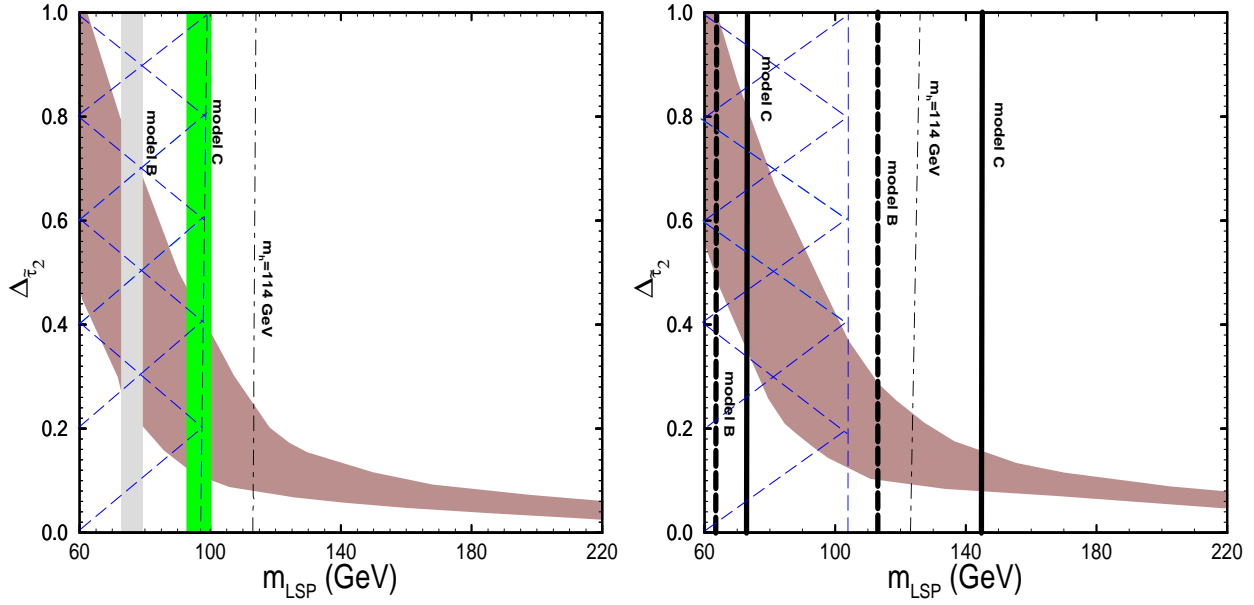


FIG. 3. The cosmologically allowed region in the $m_{\tilde{\chi}} - \Delta_{\tilde{\tau}_2}$ plane (shaded area) for $\tan \beta = 40$ (left) and $\tan \beta = 52$ (right). The vertical bands in graph on the left correspond to the bound $\sigma_{scalar}^{(nucleon)} = 4 \cdot 10^{-7} pb$, obtained from figure 2 for both models. The vertical lines on the graph of the right correspond to the bounds $\sigma_{scalar}^{(nucleon)} = 4 \cdot 10^{-7} pb$ (lines towards the right of the graph) and $2 \cdot 10^{-5} pb$ for the models indicated. The marked areas on the left are excluded by $b \rightarrow s\gamma$.

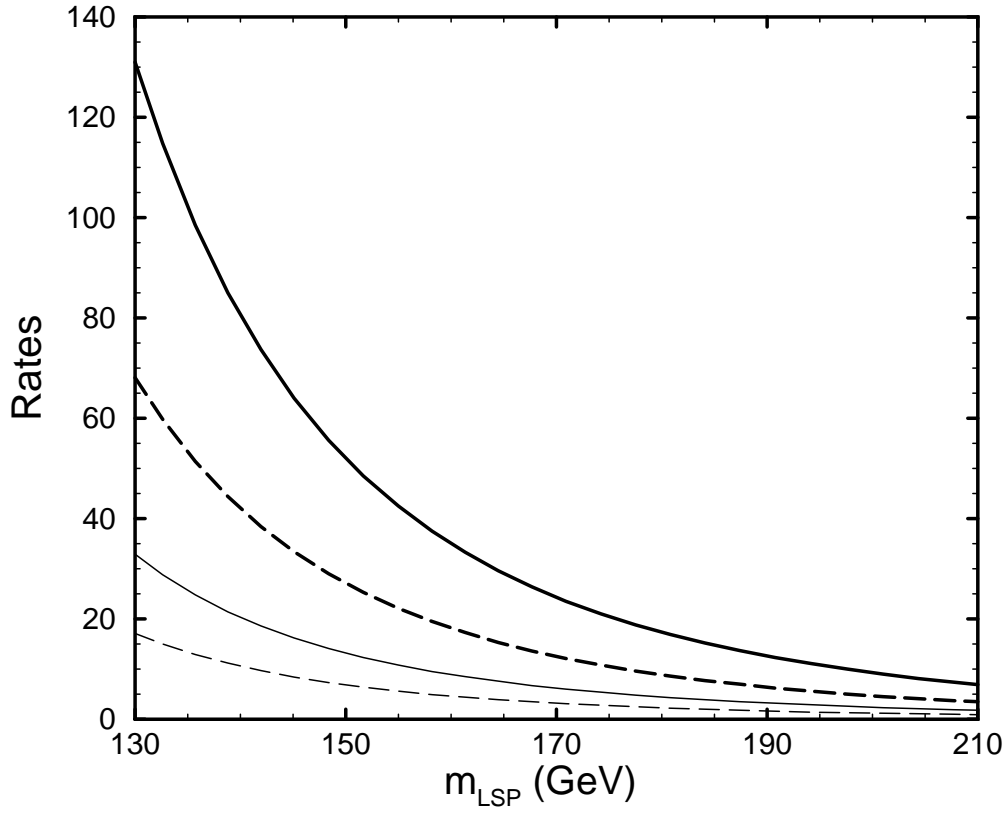


FIG. 4. The Total detection rate per $(kg - target)yr$ vs the LSP mass in GeV in the case of ^{127}I , corresponding to model B (thick lines) and Model C (fine lines). We used the parameter space corresponding to $\tan \beta = 52$ and $m_h > 114$ GeV. On the solid curves we used no detector threshold energy cut off. On the dashed ones, the value 10 KeV was employed.